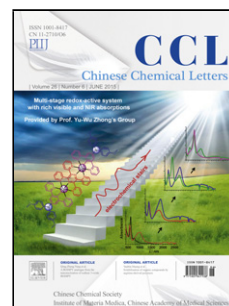# Accepted Manuscript

Title: Functionality proportion and corresponding stability study of multivariate metal-organic frameworks

Authors: Jie Li, Yecheng Wang, Yan Yu, Qiaowei Li

Please cite this article as: Jie Li, Yecheng Wang, Yan Yu, Qiaowei Li, Functionality proportion and corresponding stability study of multivariate metal-organic frameworks, Chinese Chemical Letters https://doi.org/10.1016/j.cclet.2017.12.026

Communication

Functionality proportion and corresponding stability study of multivariate metal-organic frameworks

Jie Li[a], Yecheng Wang[b], Yan Yu[c], Qiaowei Li[a],[*]

[a] *Department of Chemistry, iChEM (Collaborative Innovation Center of Chemistry for Energy Materials), and Shanghai Key Laboratory of Molecular Catalysis and Innovative Materials, Fudan University, Shanghai 200433, China*
[b] *State Key Laboratory of Coordination Chemistry, School of Chemistry and Chemical Engineering, Nanjing University, Nanjing 210023, China*
[c] *School of Physical Science and Technology, ShanghaiTech University, Shanghai 201210, China*

Graphical Abstract

BDC-NH$_2$ MTV-MOFs Zn$_4$O(BDC)$_x$(BDC-NH2)$_{3-x}$ BDC

Thermal and chemical stability
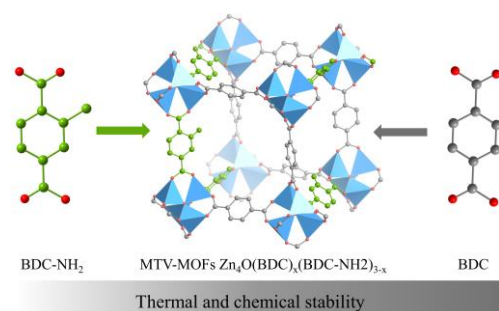
Zn-based multivariate metal-organic frameworks (MTV-MOFs) with different functionality proportions and with different thermal and chemical stabilities can be obtained by employing the appropriate synthesis method.

ARTICLE INFO

ABSTRACT

Multivariate metal-organic frameworks (MTV-MOFs) with different ratios of terephthalate (BDC) linker and amino-benzenedicarboxylate (BDC-NH$_2$) linker were synthesized through both direct synthesis from linker mixture and linker exchange of activated single-linker MOFs. Functionality proportion was impacted by the thermodynamics during the one-pot MOF construction, resulting in preference of BDC over BDC-NH$_2$ in the MTV-MOF, in agreement with the quantum mechanics calculations. The functionality difference also affects the thermodynamics in the linker exchange process, as indicated by the more effective linker exchange in BDC-NH$_2$-based IRMOF-3 than in BDC-based MOF-5. Furthermore, the thermal decomposition temperatures and chemical integrity upon ambient air exposure of these MOFs with variate functionalities were investigated, and it reveals that higher proportion of BDC in the MTV-MOF crystals contribute to both higher thermal and higher chemical stabilities.

The family of metal-organic frameworks (MOFs) [1-3] has greatly extended after the discovery of multivariate metal-organic frameworks (MTV-MOFs) that maintain the same topology of the crystals with multiple metal ions or organic linkers [4-6]. MTV-MOFs provide a platform to adjust the proportion of the functionalities without losing order, which makes them promising materials for gas adsorption [7] and catalysis [8-11] by providing different functionalities that could work together and complement each other.

[*] Corresponding author.
 E-mail address: qwli@fudan.edu.cn

The functionality proportion in MTV-MOFs is of great importance because it decorates the chemical environments around the pore channels inside the crystals, and can thus affect some important material properties [12], such as thermal and chemical stabilities. The capability of selecting different linkers with different ratios while keeping the single crystallinity with specific topology allows us to elucidate the relationship between the functionality proportion and the corresponding thermal and chemical stabilities in the MOFs.

In this report, Zn-based MTV-MOFs with two distinct linkers: Terephthalic acid (BDC) and 2-amino-1,4-benzenedicarboxylic acid (BDC-NH_2) were synthesized with two methods, namely direct synthesis and linker exchange. The two linkers are close in length and have the same carboxylate group in both ends, which make similar coordination mode in MOF assembly, thus single crystal structures are expected for the MTV-MOFs synthesized from both methods. Functionality proportion was characterized by proton nuclear magnetic resonance (^{1}H NMR) after solid digestion and it revealed a preference of BDC in the MTV-MOF crystals, confirming that BDC linkers were thermodynamically more favored in the MOF construction. This preference is further validated by the calculation of single point energy (SPE) change in the formation of single linker MOFs (MOF-5 [1] and IRMOF-3 [13]) from starting materials, as indicated by a 54.6 kJ/mol lower energy for the formation of MOF-5 based on pure BDC compared to IRMOF-3 based on pure BDC-NH_2. Following the linker exchange route, a higher proportion of BDC than BDC-NH_2 was achieved, no matter whether the pristine MOF was MOF-5 or IRMOF-3. This is in agreement with the calculation results that MOF-5 was more resistant to linker exchange than IRMOF-3. Furthermore, the relationship between the thermal and chemical stability of the crystals and the functionality proportion was carefully investigated by evaluating the thermal decomposition temperatures and chemical integrity upon ambient air exposure of MOFs with variate functionalities. It reveals that higher proportion of BDC in the MTV-MOF crystals contribute to both higher thermal and higher chemical stabilities, suggesting a facile strategy in enhancing MOF's stability with various functionalities.

Specifically, two different methodologies were employed for the synthesis of MTV-MOFs to explore the differences in functionality proportion and crystal quality. In the first method which is direct synthesis, MTV-MOFs based on BDC and BDC-NH_2 with three different linker ratios (Fig. 1a), namely 3:1, 1:1 and 1:3 (denoted as MOF-5M-X, X=3:1, 1:1, 1:3), were obtained by heating a solution of *N,N*-diethylformamide (DEF) with Zn(NO_3)$_2$ and organic linkers with different ratios (see the Supporting information for details). MOF-5 and IRMOF-3 were also synthesized with one type of linker in the starting materials. While in the second method which is linker exchange, pristine MOF-5 (Fig. 1c) or IRMOF-3 (Fig. 1d) was immersed in a DEF solution of BDC-NH_2 or BDC with the same concentration, under 100 °C and for 48 h to produce linker-exchanged MOF-5E-a and MOF-5E-b, respectively. A high concentration of the second linker (40 mmol/L) in the solution ensures that the reaction is favorable for the formation of MTV-MOFs [14]. In addition, mild reaction condition with lower temperature but longer time is used to decrease the possibility of dissolution and reassembly towards single-linker MOFs [15], and to ensure the completeness of the exchange process. With these two strategies, MTV-MOFs with fine-tuned proportions of BDC and BDC-NH_2 distributed throughout the whole crystals were successfully obtained.
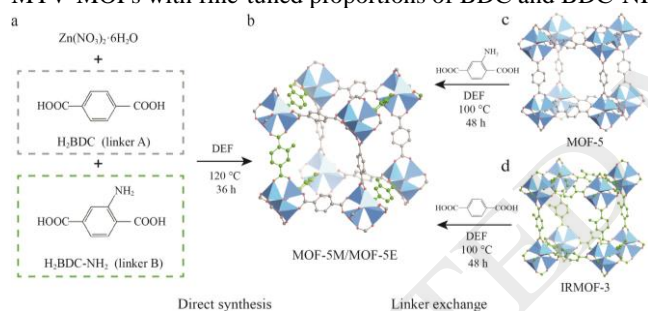

Fig. 1. Illustration of the synthesis of MTV-MOFs by both direct synthesis from linker mixture and linker exchange method from MOF-5 and IRMOF-3. Blue tetrahedra with red vertices represent the inorganic building units. BDC and BDC-NH_2 linkers are shown in gray and green, respectively.

Powder X-ray diffraction (PXRD) analysis and ^{1}H NMR analysis on the digested MOF samples were employed to investigate the structural integrity and crystallinity, and functionality proportions. Before measuring their PXRD patterns, the samples were solvent exchanged with dichloromethane and activated *in vacuo* at room temperature overnight, and the results of the PXRD analysis were given in Fig. 2. PXRD patterns of MOF-5M-X, IRMOF-3, and MOF-5E-a were almost the same as the simulated pattern of MOF-5. This result shows that the same unit cell parameters in MOF-5 with the *pcu* topology are preserved in these multivariate MOFs. However, the PXRD pattern of MOF-5E-b shows several extra peaks compared to that of MOF-5, indicating that new phases formed during the linker exchange process.
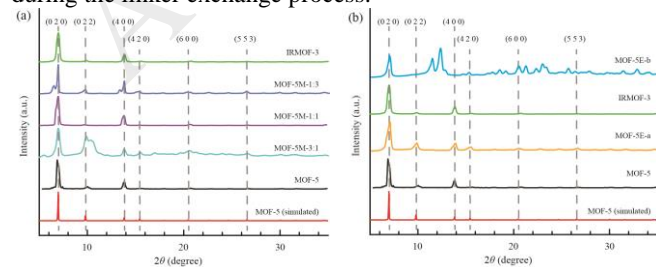

Fig. 2. PXRD patterns of (a) all the direct synthesized MTV-MOFs, single linker MOFs and simulated MOF-5, and (b) linker-exchanged MTV-MOFs, single linker MOFs and simulated MOF-5.

To quantify the amount of different linkers in MTV-MOFs, the crystals were digested with DCl in D_2O followed by measuring their ^{1}H NMR spectra (Figs. S8-S13 in Supporting information), and the functionality proportions were determined from integrating the characteristic peaks of the linkers in the spectra. The results were given in Table 1. In all the MTV-MOF samples, characteristic peaks for both BDC and BDC-NH_2 were found, suggesting two linkers were successfully integrated into the same crystal. Interestingly, a slightly higher ratio of BDC to BDC-NH_2 was discovered compared to the ratio in the starting materials of MOF-5M-X. The NMR results also showed a higher amount of BDC (64.4%) than BDC-NH_2 in MOF-5E-a, and the proportion of BDC linkers is even higher in MOF-5E-b (77.9%).

Table 1

Linker ratios in different MTV-MOFs.

Sample name	Linker proportion	
	BDC (%)	BDC-NH_2 (%)
MOF-5	100	0
MOF-5M-3:1	79.1	21.9
MOF-5M-1:1	58.0	42.0
MOF-5M-1:3	29.1	70.9
IRMOF-3	0	100
MOF-5E-a	64.4	35.6
MOF-5E-b	77.9	22.1

The reason why BDC is more preferable in the crystals could be due to different crystal growth rates [16]. In this way, the ratio of the two linkers in the sample under different reaction times should be different. However, it has already been shown that the linker ratio does not vary dramatically in concern of reaction time [5]. Therefore, it was thermodynamics rather than kinetics that contributed to the preference of BDC in the crystals. The electron-donating character of amine group in BDC-NH_2 and the hydrogen bond formed between the H in the carboxylic group and the N in amine group made BDC-NH_2 (pK_a = 3.95) less acidic than BDC (pK_a = 3.52). Therefore, the feasible deprotonation [1] assists the assembly of the linker with metal ions to form single crystals. In addition, the steric effects of the amino group could hinder BDC-NH_2 from getting into the MOFs.

To further inspect the thermodynamic differences when the two linkers are coordinated with the metal, we use the reaction of pristine MOF-5 and IRMOF-3 as the simplified models for single point energy (SPE) calculation. The energy differences between the obtained products and their corresponding starting materials were calculated with the DMol3 module in Materials Studio [17-21] using GGA-PBE functional [22] (more details of the calculations can be found in the Supporting information). This quantum mechanics calculation provides a sufficiently accurate thermodynamic description of the procedure. As a result, the formation of MOF-5 from BDC is 54.6 kJ/mol more exothermic than the formation of IRMOF-3 from BDC-NH_2, and it suggests that the participation of BDC in the crystal formation is more thermodynamically favored compared to BDC-NH_2, which is in consistence with our experiment observation.

The morphology and the crystal quality change during the synthesis provides a closer look on the different reaction mechanisms with two synthetic methods. Single crystals of MOF-5, IRMOF-3, MOF-5M-X, and MOF-5E-X were carefully inspected under the optical microscope, and the results were given in Fig. 3 and Figs. S19-S25 (Supporting information). MOF-5M-X crystals obtained from direct synthesis were translucent uniformly, indicating the two linkers were evenly distributed without any macroscopic domains in the crystals. With the percentage of BDC-NH_2 increasing in the crystal, the color of the crystals becomes darker. On the other hand, the MOF-5E-X crystals obtained from linker exchange process were more heterogeneous in terms of color uniformity than direct synthesized crystals. As shown in Fig. 3d, MOF-5E-a exposed a gradient of transparency from outside to inside, while retaining their original cubic shapes. That means, BDC-NH_2 was more concentrated on the surface of the crystals, contributing to the darker shell. Linker exchange in the inner parts of the crystals requires the diffusion of BDC-NH_2 linker into the core and the reorganization near the exchange sites, leading to the impedance in the linker exchange in the core. However, in the case of MOF-5E-b, a large quantity of small colorless crystals were found in the suspension as well as on the surface of cubic crystals. This explains the peaks not corresponding to MOF-5 in PXRD (Fig. 2b). The small crystal size limits the single crystal X-ray diffraction studies on this new phase; however, a preliminary digested NMR study shows that the new crystals were formed with BDC and Zn^{2+} after the dissolution of some IRMOF-3 frameworks, and only negligible amount of BDC-NH_2 was detected (Fig. S13 in Supporting information). Overall, the appearances of these crystals demonstrate that linker exchange method is a facile strategy to build linker composition gradient within each piece of single crystals, despite that the dissolution-recrystallization may be a hindrance for the application of linker exchange.
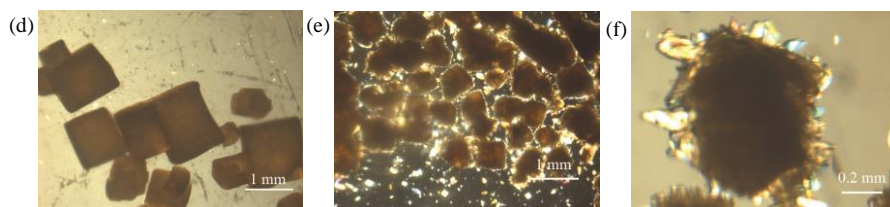
(a)
(b)
(c)

Fig. 3. Optical microscope images of (a) MOF-5, (b) MOF-5M-1:1, (c) IRMOF-3, (d) MOF-5E-a, (e) MOF-5E-b, and (f) a magnified image of small crystals on the surface of MOF-5E-b.

In the linker exchange experiments performed, we obtain higher exchange yield in the case of IRMOF-3 (77.9% BDC-NH$_2$ was replaced by BDC) compared to MOF-5 (35.6% BDC was replaced by BDC-NH$_2$). This intrigued us to examine how easily linkers could be exchanged from MOF-5 and IRMOF-3. The whole procedure of linker exchange would begin from exchanging the first linker from the crystal. Hence, calculations on SPE changes during one linker exchange in each unit cell of MOF-5 and IRMOF-3 were investigated. The results showed a 37.2 kJ/mol energy rise for one BDC-NH$_2$ replacing one BDC in a MOF-5 unit cell, and only 2.49 kJ/mol in the case of BDC replacing BDC-NH$_2$ in IRMOF-3. Details of the simulation are given in the Supporting information. The result revealed that more energy was needed for MOF-5 to undergo linker exchange, resulting in less exchange yield for linker exchange in MOF-5, which is in accordance with the experimental results.

With the MTV-MOFs with various proportions of BDC and BDC-NH$_2$ in hand, we were interested in the relationship between the composition and their thermal stability. The thermal stabilities of MOF-5, IRMOF-3, and MOF-5M-X were tested by the thermogravimetric analysis (TGA) from room temperature to 700 $^{\circ}$C under a heating rate of 10 $^{\circ}$C/min in air. As shown in Fig. 4a, all the five samples showed only one stage of decomposition, during which about 50% of the mass was lost, with the ultimate product of decomposition being ZnO [23]. MOF-5 has the highest decomposition temperature of 520 $^{\circ}$C among the five samples, while the least thermally stable MOF in this series (IRMOF-3) would decompose at 432 $^{\circ}$C, which is 88 $^{\circ}$C lower than that of MOF-5. All the MOF-5M-X decomposed at temperatures lower than that of MOF-5 but higher than that of IRMOF-3. More interestingly, a linear relationship between the decomposition temperature and the actual linker proportion in MOF-5M-X was revealed (Fig. 4b). This study shows that it is reasonable to predict the thermal stability of MTV-MOFs based on the TGA on the corresponding single-linker isoreticular MOFs.
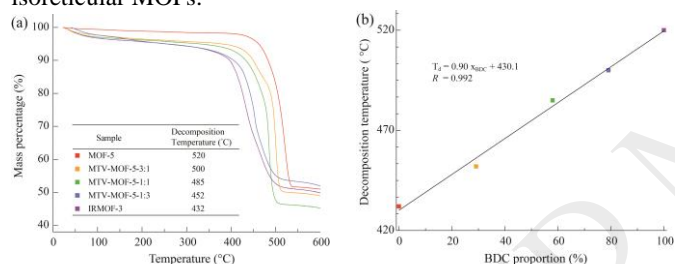

Fig. 4. (a) TGA curves for MOF-5, IRMOF-3, and MOF-5M-X. Decomposition temperatures are defined as the temperature corresponding to the maximum in the first derivative of the TGA curves. (b) Relationship between MOF-5M-X decomposition temperature (T_d) and actual BDC proportion (x_{BDC}) in the crystals.

MOF-5 shows relatively low chemical stability when they were exposed to the ambient air, mainly caused by the H$_2$O that interacts with metal ions in the MOF [24]. The decomposition is usually accompanied by a change in the appearance of the crystals due to a decrease in crystal quality [25], Thus the appearance snapshots of the crystals during exposure in the air is a straightforward indicator of the chemical stability of a MOF. We picked MOF-5, MOF-5M-1:1, and IRMOF-3 as three examples in the MTV-MOF series. Specifically, activated MOF-5 and IRMOF-3 crystals with similar size were exposed to the air under the same conditions, and their appearances over time were recorded under optical microscope (Fig. 5). As expected, both MOF crystals eventually turned opaque when exposed to the air, mainly attributed by the interaction between [Zn$_4$O(COO)$_3$]$^{3+}$ building blocks in both MOFs with atmospheric water [26]. However, the time scale was different for both MOFs when they turned opaque. Within the same time of 420 s, IRMOF-3 crystals had completely turned opaque (Fig. 5b), while MOF-5 crystals were mostly translucent overall (Fig. 5e). The decomposition of MOF-5 continued after 420 s, as evidenced by the opacity increase with time until 1380 s. The decomposition of MOF-5M-1:1 was found to be slower than MOF-5, but still faster than IRMOF-3 (Fig. S28 in Supporting information).
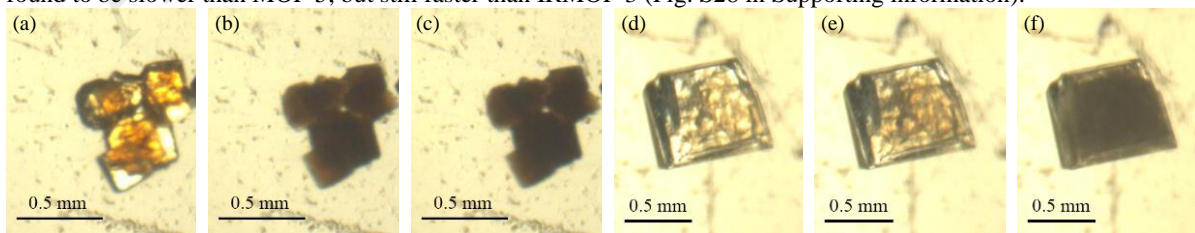

Fig. 5. Optical microscope images of MOF decomposition for (a) IRMOF-3, t = 0 s, (b) IRMOF-3, t = 420 s, (c) IRMOF-3, t = 540 s, (d) MOF-5, t = 0 s, (e) MOF-5, t = 420 s, (f) MOF-5, t = 1380 s.

This stability difference can be explained by the organic functionality discrepancy between the two MOFs. The amine groups of BDC-NH_2 in IRMOF-3 form hydrogen bonds with H_2O molecules, making H_2O in close distance with the $[Zn_4O(COO)_3]^{3+}$ secondary building unit, providing more possibility of strong interactions between them. Better stability could be achieved by using linkers with more hydrophobicity, such as 2-trifluoromethylterephthalic acid or dimethylterephthalic acid [27]. In addition, considering the synergetic effects between different linkers in one MOF, it is possible to synthesize MTV-MOFs that are more stable than any of the single-linker MOFs, because the properties of MTV-MOFs may be better than the linear combination of each linker in the product [28].

In summary, MTV-MOFs with BDC and BDC-NH_2 were synthesized through two methods. Using direct synthesis from linker mixture, the proportion of each linker in the MOF could be precisely controlled by the linker ratio in the starting material. By performing linker exchange on the activated single-linker MOFs, different linker distribution from direct method was observed, which promises them different applications. Calculation on the MOF-5 and IRMOF-3 revealed that MOFs with BDC are thermodynamically more stable than those with BDC-NH_2, and more difficult to be linker-exchanged. TGA reveals the linear relationship between the MTV-MOF's decomposition temperature with the linker proportion in the crystal, and higher percentage of BDC results in higher thermal stability. What is more, the functional group's role in the chemical stability of the MOFs were studied. Hydrophilic amine groups in the organic linker reduces the moisture susceptibility in IRMOF-3 compared to MOF-5. With the potential synergetic effects brought by multiple linkers, MTV-MOFs with controllable functionality proportion and distribution provides a tool box for designing functional materials with specific thermal and chemical stability.

References

[1] H. Li, M. Eddaoudi, M. O'Keeffe, O.M. Yaghi, Nature 402 (1999) 276-279.
[2] S. Kitagawa, R. Kitaura, S. Noro, Angew. Chem. Int. Ed. 43 (2004) 2334-2375.
[3] G. Férey, Chem. Soc. Rev. 37 (2008) 191-214.
[4] H. Furukawa, U. Müller, O.M. Yaghi, Angew. Chem. Int. Ed. 54 (2015) 3417-3430.
[5] H. Deng, C.J. Doonan, H. Furukawa, et al., Science 327 (2010) 846-850.
[6] A. Helal, Z.H. Yamani, K.E. Cordova, O.M. Yaghi, Natl. Sci. Rev. 4 (2017) 296-298.
[7] Y.B. Zhang, H. Furukawa, N. Ko, et al., J. Am. Chem. Soc. 137 (2015) 2641-2650.
[8] D. Ma, B. Li, Z. Shi, Chin. Chem. Lett. (2017) DOI: 10.1016/j.cclet.2017.09.028.
[9] Y. Chen, Z.U. Wang, H. Wang, et al., J. Am. Chem. Soc. 139 (2017) 2035-2044.
[10] G. Cai, W. Zhang, L. Jiao, S.H. Yu, H.L. Jiang, Chem. 2 (2017) 791-802.
[11] X. Ni, J. Liu, Y. Liu, et al., Chin. Chem. Lett. 28 (2017) 1057-1061.
[12] C.R. Wade, T. Corrales-Sanchez, T.C. Narayan, M. Dincă, Energy Environ. Sci. 6 (2013) 2172-2177.
[13] M. Eddaoudi, J. Kim, N. Rosi, et al., Science 295 (2002) 469-472.
[14] A.F. Gross, E. Sherman, S.L. Mahoney, J.J. Vajo, J. Phys. Chem. A 117 (2013) 3771-3776.
[15] O. Karagiaridi, W. Bury, J.E. Mondloch, J.T. Hupp, O.K. Farha, Angew. Chem. Int. Ed. 53 (2014) 4530-4540.
[16] A.D. Burrows, L.C. Fisher, C. Richardson, S.P. Rigby, Chem. Commun. 47 (2011) 3380-3382.
[17] B. Delley, J. Chem. Phys. 92 (1990) 508-517.
[18] J. Baker, A. Kessi, B. Delley, J. Chem. Phys. 105 (1996) 192-212.
[19] B. Delley, J. Chem. Phys. 100 (1996) 6107-6110.
[20] B. Delley, J. Chem. Phys. 113 (2000) 7756-7764.
[21] B. Delley, J. Phys. Condens. Matter 22 (2010) 384208.
[22] J.P. Perdew, K. Burke, M. Ernzerhof, Phys. Rev. Lett. 77 (1996) 3865-3868.
[23] L. Zhang, Y.H. Hu, J. Phys. Chem. C 114 (2010) 2566-2572.
[24] M. Bosch, M. Zhang, H.C. Zhou, Adv. Chem. 2014 (2014) 1-8.
[25] G. Dhanaraj, K. Byrappa, V. Prasad, M. Dudley, Springer Handbook of Crystal Growth, Springer, Berlin, 2010.
[26] S.S. Kaye, A. Dailly, O.M. Yaghi, J.R. Long, J. Am. Chem. Soc. 129 (2007) 14176-14177.
[27] T. Wu, L. Shen, M. Luebbers, et al., Chem. Commun. 46 (2010) 6120-6122.
[28] T.M. Osborn Popp, O.M. Yaghi, Acc. Chem. Res. 50 (2017) 532-534.